Selective Separation of Similarly Sized Proteins with Tunable Nanoporous Block Copolymer Membranes

Xiaoyan Qiu,[†] Haizhou Yu,[†] Madhavan Karunakaran,[†] Neelakanda Pradeep,[†] Suzana P. Nunes,[‡] and Klaus-Viktor Peinemann[†,*]

[†]Advanced Membranes and Porous Materials Center and [‡]Water Desalination and Reuse Center, 4700 King Abdullah University of Science and Technology (KAUST), Thuwal 23955-6900, Kingdom of Saudi Arabia

ABSTRACT An integral asymmetric membrane was fabricated in a fast and one-step process by combining the self-assembly of an amphiphilic block copolymer (PS-*b*-P4VP) with nonsolvent-induced phase separation. The structure was found to be composed of a thin layer of densely packed highly ordered cylindrical channels with uniform pore sizes perpendicular to the surface on top of a nonordered sponge-like layer. The as-assembled membrane obtained a water flux of more than 3200 L m^{-2} h^{-1} bar^{-1}, which was at least an order of magnitude higher than the water fluxes of commercially available membranes with comparable pore sizes, making this membrane particularly well suited to size-selective and charge-based separation of biomolecules. To test the performance of the membrane, we conducted diffusion experiments at the physiological pH of 7.4 using bovine serum albumin (BSA) and globulin-γ, two proteins with different diameters but too close in size (2-fold difference in molecular mass) to be efficiently separated *via* conventional dialysis membrane processes. The diffusion rate differed by a factor of 87, the highest value reported to date. We also analyzed charge-based diffusive transport and separation of two proteins of similar molecular weight (BSA and bovine hemoglobin (BHb)) through the membrane as a function of external pH. The membrane achieved a selectivity of about 10 at pH 4.7, the isoelectric point (pI) of BSA. We then positively charged the membrane to improve the separation selectivity. With the modified membrane BSA was completely blocked when the pH was 7.0, the pI of BHb, while BHb was completely blocked at pH 4.7. Our results demonstrate the potential of our asymmetric membrane to efficiently separate biological substances/pharmaceuticals in bioscience, biotechnology, and biomedicine applications.

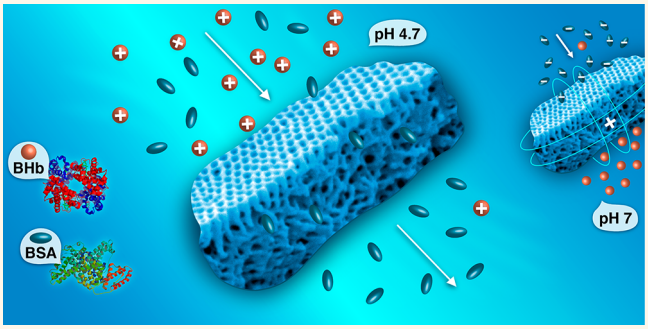

KEYWORDS: block copolymer membranes · self-assembly · phase separation · selective protein separation · quaternization

Existing processes for bioseparations using conventional resin-based chromatography are time-consuming and expensive.[1,2] Newly developed membrane separation processes offer substantial economic, environmental (less energy consumption), and safety benefits.[3,4] Micro/nanofabricated membranes with various pore sizes, lengths, morphologies, and densities have been synthesized from diverse inorganic, organic, and composite materials.[5−9] Studies of nanostructured membranes have demonstrated their great potential in biomolecule separation applications.[10−12] Size-based separation of proteins can be carried out by ultrafiltration membrane systems when the proteins have significantly different molecular sizes.[13−16] However, separation of similar-sized proteins with current commercially available membranes is not possible.[17] Recently, Striemer *et al.*[5] have reported the fabrication of porous nanocrystalline silicon (pnc-Si) membranes using standard silicon fabrication techniques. Their ultrathin membrane had average pore sizes ranging from 5 to 25 nm and a thickness of only 15 nm. Using their membrane, they demonstrated the separation of BSA (66 kDa) from immunoglobulin-γ (IgG; 150 kDa), two proteins that have only a 2-fold difference in molecular weight (MW). They found that BSA diffused through the membrane four times more quickly than IgG did, which was a significant improvement over conventional dialysis membranes that are able to separate proteins with at least a 10-fold difference in MW. However, their membrane had an area of

* Address correspondence to klausviktor.peinemann@kaust.edu.sa.

Received for review October 31, 2012 and accepted December 19, 2012.

Published online December 19, 2012
10.1021/nn305073e

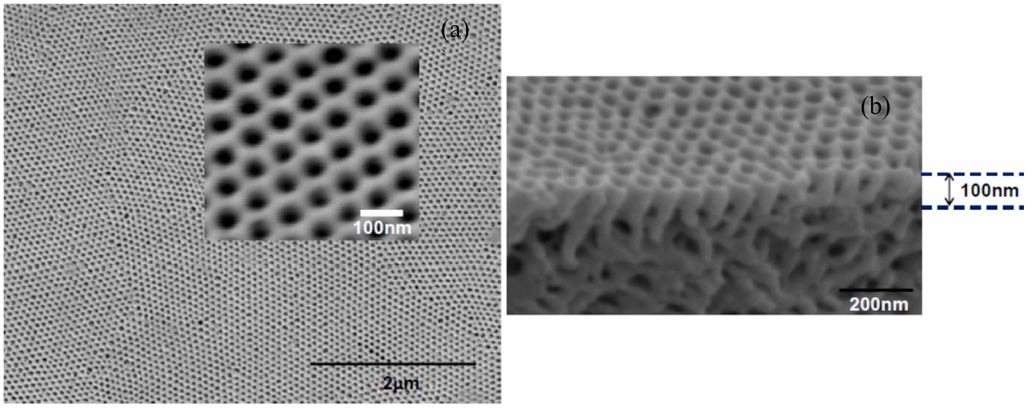

Figure 1. (a) Regular order of the membrane's surface as shown by SEM. (b) Cross-section SEM image showing the thin top layer and the sponge-like bottom layer.

only 0.04 mm^2, which would make it difficult to scale up its manufacture. Chun *et al.*[18] reduced the pore size of track-etched polycarbonate membranes by electroless gold deposition. The surface of the membrane was further modified and negatively charged with self-assembled monolayers (SAMs) of functionalized thiols ($HSC_{10}H_{20}COOH$). With this PCTE/Au/SAMs membrane, they separated two similar-sized proteins, bovine serum albumin (BSA) and bovine hemoglobin (BHb), with an ionic strength difference (to cause osmotic flow) in a U-shaped diffusion cell. They obtained a separation factor of 4.2 at pH 4.7, which corresponds to the isoelectric point of BSA. Two years later, they used the same membrane for the separation of these two proteins again with a much lower ionic strength.[19] Although they achieved a higher separation selectivity of about 67, the complicated procedures and low pore density (6 pores/μm^2) could limit the use of the membranes.

Here, we fabricated an integral asymmetric membrane by combining the self-assembly of an amphiphilic block copolymer (PS-*b*-P4VP) and nonsolvent-induced phase separation.[20,21] We found that the membrane was composed of a thin layer of densely packed, highly ordered cylindrical channels with uniform pore sizes perpendicular to the surface on top of a nonordered, sponge-like layer. Due to the pore density and the thin top layer, the water flux through the membrane was more than 3200 L m^{-2} h^{-1} bar^{-1}, which was almost 2 orders of magnitude higher than the water fluxes of commercially available membranes with comparable pore sizes. Another remarkable property of this membrane is that it is stimuli (pH)-responsive. These attractive characteristics make this membrane particularly suitable for applications that require size-selective and charge-based separation of biomolecules. Biomolecule transport through this type of asymmetric self-assembled membrane has not previously been studied. With our membrane we efficiently separated similar-sized proteins with high selectivity. We further modified the whole membrane (not only the surface) by quaternization to improve the separation selectivity of two similar-sized proteins. In this study, we report on the separation mechanism of PS-*b*-P4VP membranes with tunable pore sizes and charges.

RESULTS AND DISCUSSION

Membrane Preparation and Morphology Characterization. We recently described the use of supramolecular assemblies of block copolymer micelles in solution in the presence of copper ions for the manufacture of asymmetric membranes with thin nanoporous top layers (400 nm thickness).[22,23] Here we used a block copolymer with a different block ratio and dissolved in a different solvent mixture. We obtained an asymmetric membrane by combining the self-assembly of an amphiphilic block copolymer (PS-*b*-P4VP) with nonsolvent-induced phase separation. We found that the membrane had very dense and highly ordered cylindrical channels with uniform pore sizes perpendicular to the surface on top of a nonordered sponge-like layer. The diameter of the very regular pores was approximately 34 nm measured from SEM images at high magnification. It should be mentioned that the effective pore diameter would actually be smaller, because the pores were lined with P4VP. The regular order of the monodispersed nanopores was also confirmed by SEM images (Figure 1a). The pore density on the surface, as shown in Figure 1, was estimated to be around 2.2×10^{14} pores per square meter. The average cylinder length of the well-ordered top layer as shown in the cross-section SEM image (Figure 1b) was around 100 nm, which was much smaller than the 400 nm that we were previously able to obtain.[22,23] This tiny cylinder length allowed unmatched water flux through the membrane. The area of an as-produced membrane was more than 50 cm^2, which made it easy to handle and use. Scale up to m^2 production would be possible on conventional membrane casting machines.

Water Flux and pH Response Characterization. The membrane water flux as a function of pH is shown in Figure 2 (green curve), indicating its particularly strong response

to pH. The fluxes at low pH (below 4) were very small. The pyridine groups at the membrane surface and pore walls were protonated at low pH, and the P4VP segments stretch to minimize charge repulsion, transforming the pores into a pH-sensitive gate. Very high water fluxes of more than 3200 L m^{-2} h^{-1} bar^{-1} were obtained in this study in the middle pH range of 6–8, which were an order of magnitude greater than the fluxes of commercial membranes with similar pore sizes. The water fluxes were a consequence of the exceptional porosity and the reduced thickness of the top separation layer.

Under the assumption that the main flow resistance was in the 100 nm ordered top layer, Hagen–Poiseuille's law can be used to give an estimate of the effective pore size corresponding to the measured water flux through the membrane:

$$dv/dt = (\pi R^4 \Delta p)/(8\eta L)$$

where R is the pore radius, Δp is the pressure drop through the membrane, η is the water viscosity (8.9×10^{-4} Pa s at 25 °C), and L is the length of the pores.

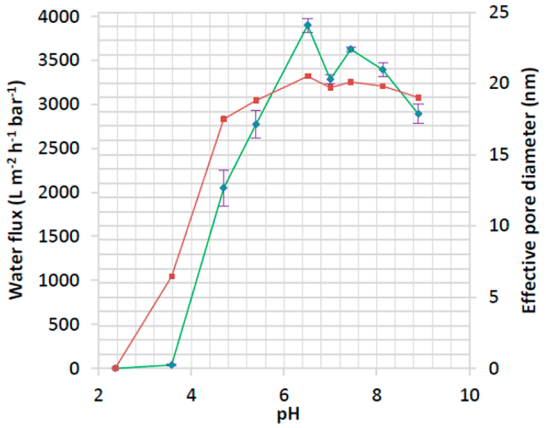

Figure 2. Water fluxes (green) and effective pore diameters (red) of the pH-responsive nanoporous membrane, measured at 1.38 bar feed pressure.

In Figure 2 (red curve) the pore diameters estimated by the Hagen–Poiseuille equation are shown as a function of pH. Practically no hysteresis of the water flux was observed when the pH was increased or decreased, suggesting that the pores can reversibly close or open. The cyclability of the membranes was confirmed at a large number of cycles. This stimuli (pH)-responsive membrane with tunable nanopores can be used as a sensitive gate controlled by pH without any modification.

Size-Selective Experiments at Physiological pH. To measure the membrane's separation capability based on size difference, we used two proteins with different molecular weights and diameters (D): bovine serum albumin (MW = 67 kDa, D = 6.8 nm) and globulin-γ (MW = 150 kDa, D = 14 nm). BSA and IgG are too close in size (2-fold difference in their MW) to be efficiently separated through conventional dialysis membrane processes[24] (proteins with at least a 10-fold MW difference are recommended by dialysis membrane manufacturers). Diffusive experiments at the physiological pH of 7.4 in phosphate-buffered saline (PBS) were carried out, and the passage of the two proteins was monitored. Figure 3a shows the comparison of the permeabilities of IgG and BSA at 1.0 mg/mL concentration through our membrane. It is evident that our membrane hindered the diffusion of IgG more than it hindered the diffusion of BSA by a factor of 87. An interesting finding from our diffusion experiments is that IgG was retained by the membrane with pore sizes more than twice as large as its hydrodynamic diameters. This is consistent with a previous report by Striemer *et al.*[5] It is possible that electrostatic interactions and protein adsorption might reduce the effective pore size. There are other factors that also influence the diffusion of the two proteins besides size exclusion, such as external pH, ion strength, and protein structure. These factors will be further discussed below in the experiments with BSA and BHb.

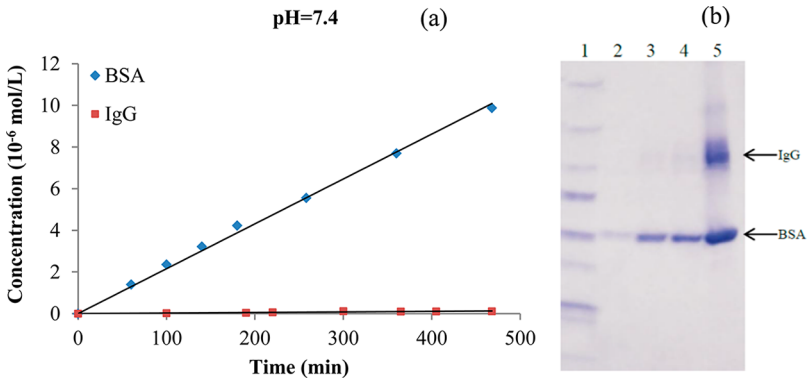

Figure 3. (a) Protein concentration in the receiving chamber measured by Bradford assay *versus* time at the physiological pH of 7.4 in PBS. (b) Results of SDS-PAGE analysis. Lane 1: 5 μL of protein molecular-weight standards; lanes 2, 3, and 4: 5 μL of protein samples collected from the right chamber after 1, 3, and 5 h, respectively; lane 5: 5 μL of initial mixed protein solution of BSA and IgG in the left chamber.

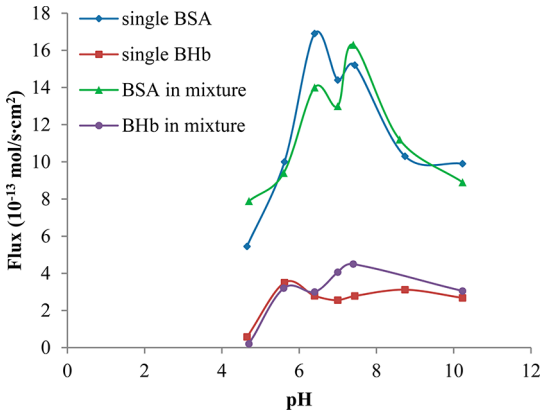

Figure 4. Average protein flux of replicates at each pH.

We confirmed the high separation selectivity of these two proteins by SDS-PAGE analysis, as shown in Figure 3b. The concentration of BSA increased gradually with time (lanes 2, 3, and 4 in Figure 3b). However, there was no appearance of IgG in lanes 2, 3, and 4, indicating that the IgG molecules did not pass through the membrane.

Single Protein Transport and Mixed Protein Separation (BSA–BHb System). It is difficult to separate BSA and BHb because of their nearly identical molecular weights (BHb 65 kDa, BSA 66 kDa), but BSA has a lower isoelectric point (pI = 4.7) than BHb (pI = 7.0). The isoelectric point of a protein plays an important role in transport. When the pH value of a buffer solution is exactly equal to the pI of a protein, the surface charge of the protein is neutral. When the pH deviates even slightly from the pI of the protein, the charge of the protein changes. At a pH above the pI, the protein is negatively charged; at a pH below pI, the protein is positively charged.

We first tested the effect of external pH on single protein transport through our membrane. The pH of the buffer solution was varied from 4.67 to 10.32, while its ionic strength in the chambers was maintained at 0.01 M. We performed each experiment at different pH in triplicate. Figure 4 shows the results of the average flux of both BSA and BHb across the membrane as a function of the external pH. Both flux curves of BSA and BHb follow an M-shaped pattern, which was already observed for the water flux (Figure 2). The flux of BSA through the membrane was much higher than the flux of BHb at all pH values tested. A 9.5-fold difference in the diffusion rate was observed at pH 4.7. Although the molecular weights of BSA and BHb are quite similar, other parameters such as the molecular shape, mobility, hydrophilic-to-hydrophobic ratio of amino acids, and the isoelectric point are different. A combination of these factors influences the protein transport behavior through the nanopores of the membrane.

The size of a BSA protein is 14 nm × 3.8 nm × 3.8 nm, and it resembles a globular prolate ellipsoid, while the size of BHb is 6.4 nm × 5.5 nm × 5 nm and its

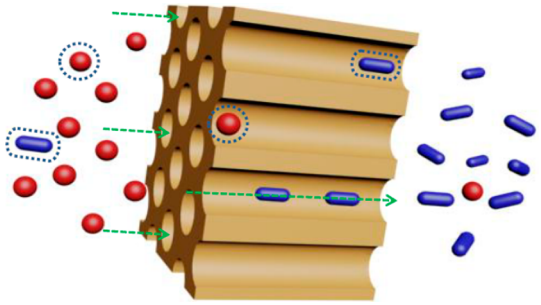

Figure 5. Schematic of the membrane that shows the transport of BSA (blue ellipsoid) and BHb (red sphere) through the membrane at pH 4.7.

shape is more sphere-like than that of BSA. In bulk diffusion, the ellipsoid BSA diffuses in all orientations, while BHb diffuses more like a sphere. This conformation effect can cause a slower mobility for BSA compared to that of BHb. The diffusion coefficient of BSA (5.9×10^{-11} m^2/s) is lower than that of BHb (6.4×10^{-11} m^2/s) in bulk solution. However, as pointed out by Chun *et al.*,[18] diffusion in narrow nanopores is quite different, especially when the pore size and protein size are close. To have the least interaction with the nanoscale pores, the ellipsoid-shaped BSA molecule might align its long axis parallel to the centerline of the nanopore, leading to lower hydrodynamic hindrance than BHb has. This alignment of BSA within the pores then causes a reduction in the hindered diffusion. In contrast, the sphere-shaped BHb interacts regardless of its alignment inside the pores. BSA therefore diffuses through the nanopores more rapidly than does BHb.

The hydrophilic-to-hydrophobic ratio of the amino acids within the two proteins also plays a role in protein transport. The hydrophilic amino acid content of BSA is 56%, while that of BHb is 44%. BSA is more hydrophilic than BHb. Since the surface and pore walls of the membrane are hydrophilic P4VP chains, this difference in amino acid content should make BSA more compatible than BHb inside the pores. BSA therefore passes much more easily through the membrane.

In addition to the above two factors, the ionic strength is also very important in protein transport since it influences the value of the electrical double layer thickness (Debye lengths). The effects of pH are more pronounced at lower ionic strengths.[25,26] In addition the lower the ionic strength, the longer the Debye length (dashed circles in Figure 5) of both protein molecules and the nanopore walls. This causes significant electrostatic interactions of the protein with the sufficiently narrow nanopores. The double layer thickness is given by[27]

$$\lambda_D = \left(\frac{\varepsilon W k_B T}{2 n_0 e^2}\right)^{1/2} \equiv (8\pi n_0 \lambda_B)^{-1/2}$$

where n_0 is the ion density (~0.006 when $I = 0.01$ M) and $\lambda_B = e^2/4\pi\varepsilon_W k_B T$ (~0.7 nm in water). We have conducted experiments at different ionic strengths. For example, at a

lower ionic strength of 0.001 M ($n_0 \approx 6 \times 10^{-4}$ ions/nm^3), the Debye length is 10 nm, which is even bigger than the protein diameters. This causes much larger electrostatic interactions of the protein molecules with the quite narrow nanopores and therefore highly decreases the protein fluxes. While the ionic strength is increased to 0.1 M ($n_0 \approx 0.06$ ions/nm^3), the Debye length is decreased to 1 nm. The separation selectivity of BSA and BHb is then decreased to around 2−3. So we choose 0.01 M as the optimum condition to get both high separation selectivity and flux. An ionic strength of 0.01 M leads to an estimated Debye length of about 3.3 nm. This is significant when compared to the protein diameter (about 6 nm) and the effective pore radius (around 11 nm) used in our studies.

Figure 4 presents a comparison of the fluxes in our mixed protein experiments with the fluxes in the single protein experiments. Clearly, the transport processes taking place in the case of the mixed protein diffusion are more complex. The fluxes for the mixed protein experiments are affected by the charge interactions between the protein molecules, their counterions, and the pore sizes in the different pH ranges. Qualitatively, the transport behavior of the proteins is similar to that of single protein diffusion. BHb exhibited a lower minimum flux at pH 4.7, while the BSA had a higher flux in the mixed protein diffusion than in the single diffusion, indicating a higher selectivity. Even though the net charge of BSA is zero at its isoelectric point, positive and negative charges are present, which suggests that neutral proteins can interact electrostatically. The presence of positive and negative charges might impart a dipole moment to the protein, which might cause the protein to interact with other charged species that influence its transport.

Furthermore, it is possible that protein clusters form (*e.g.*, dimers, trimers) that diffuse more slowly than do single molecules. Overall, the flux of BSA is still larger than that of BHb in the whole pH range.

The data presented in Figure 6 show the separation selectivity for BSA and BHb as a function of external pH. The separation selectivity S is defined as

$$S = F_{BSA}/F_{BHb}$$

where F_{BSA} and F_{BHb} are the fluxes of BSA and BHb, respectively.

In our experiments, the situation is much more complex because the protein properties and the pore size of the membrane are both sensitive to changes of pH. The highest separation selectivity of about 10 was obtained when the nanopore radius was small at pH 4.7. A decrease in the pore size should improve the separation selectivity for similar-sized proteins because it increases the ratio of Debye length to the charged protein molecule and the pore radius. Thus, controlling the external pH and ionic strength can selectively separate similarly sized proteins with the tunable membrane.

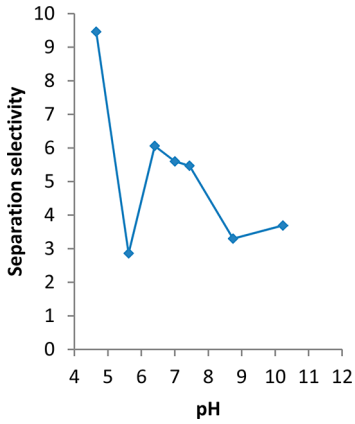

Figure 6. Separation selectivity for BSA/BHb at different pH.

Similarly Sized Protein Separation by Charged Membrane. Another critical parameter that can influence separation through nanopores is the charge of the membrane. To enhance the charge effects, the membrane was modified by quaternization. Instead of modifying only the membrane surface, we modified the whole membrane by immersing it in aqueous solutions of 2-chloroacetamide. Evidence of quaternization of the membranes was obtained from infrared (IR) spectra (Figure 7) from a FT-IR spectrometer with a new peak appearing around 1660 cm^{-1} (C═O stretch). Quaternization of poly(4-vinylpyridine) takes place quantitatively with 2-chloroacetamide. Polyvinylpyridines have been reported to be fully quaternized with 2-chloroacetamide at room temperature.[28] After quaternization the membranes were positively charged. The quantitative conversion in our study was confirmed by analysis of the chloride ions using the mercuric thiocyanate method.[29,30] From the chloride analysis it can be deduced that about 91.6% of pyridine units were quaternized after three days.

Proteins are large molecules and therefore can be heavily charged (BSA's net charge is 13− at pH 7).[14] Stronger electrostatic interactions between proteins and charged membranes were expected when the experiments were repeated with the modified membrane. Figure 8a and b show the concentrations of BSA and BHb in the right receiving cell as a function of time using pristine and quarternized membranes. We found that in low ionic strength solutions positively charged membranes completely blocked BHb at pH 4.7, while BSA rapidly passed through the membrane. This excellent selectivity resulted from the strong electrostatic repulsion of the positively charged BHb and the larger flux of the neutrally charged BSA. At this pH, BHb is highly positively charged. Thus, the BHb species were electrostatically repelled from the positively charged membrane. Moreover, a sufficiently large electrical double layer thickness should also significantly reduce the diffusion of the charged BHb. In addition, an increase in BSA transport was measured relative to that with the unmodified membrane, which also efficiently enhanced

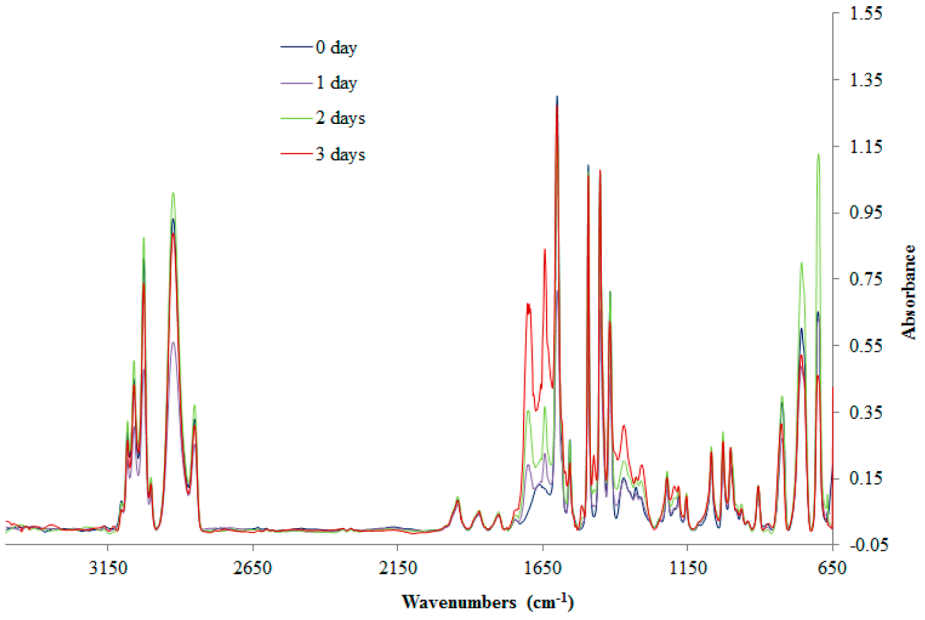

Figure 7. FT-IR spectra collected on PS-*b*-P4VP membranes after quaternization in aqueous solution of 2-chloroacetamide for different times. The new peak due to quaternization is around 1660 cm^{-1}.

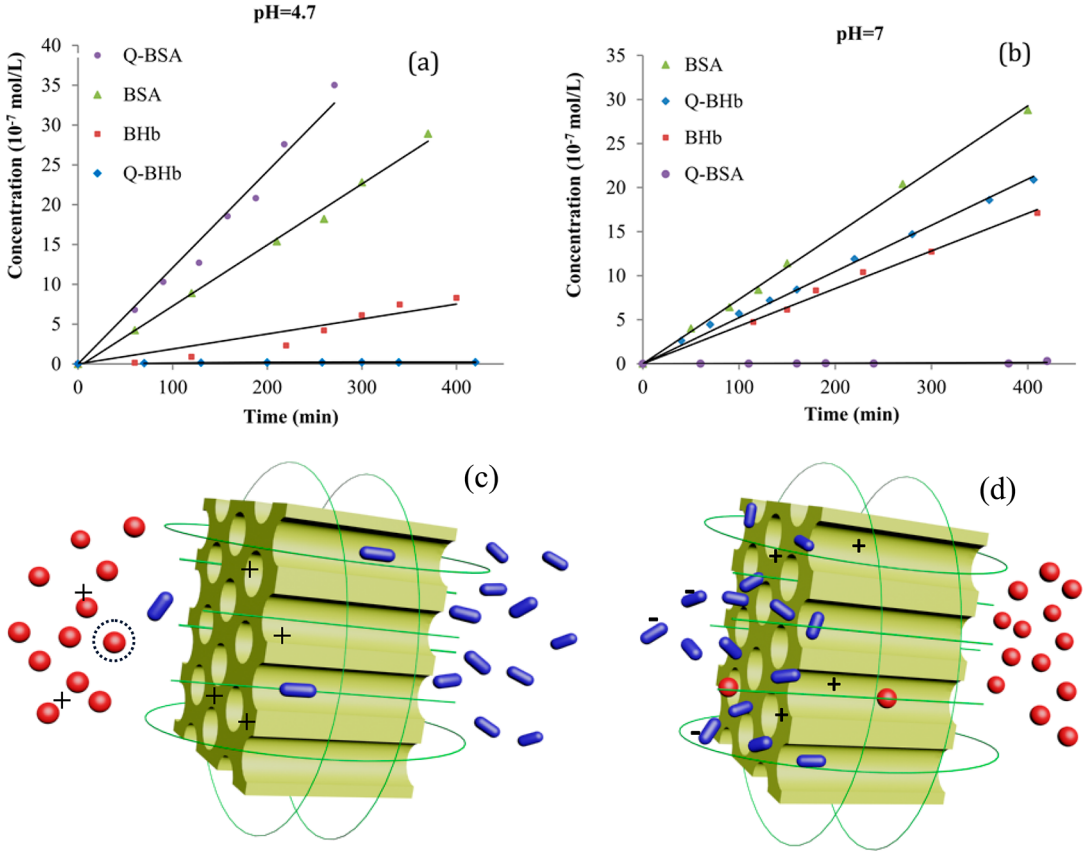

Figure 8. Concentration *versus* time for BSA and BHb at pH 4.7 (a) and pH 7 (b), *I* = 0.01 M. The schematics show the transport of BSA (blue ellipsoids) and BHb (red spheres) through the membrane at pH 4.7 (c) and pH 7 (d).

the selectivity of BSA over BHb. We interpret this as a consequence of the diffusion potential inside the nanopores caused by the electric field resulting from the membrane charge. This might disturb the charge of the neutral BSA and therefore influence its rate of transport.

In contrast, at pH 7 BSA was effectively retained by the positively charged membrane, while BHb freely passed through the membrane. The BHb diffused faster and exhibited a maximum flux at pH 7. In this case, the BHb molecules were neutral, while the BSA molecules

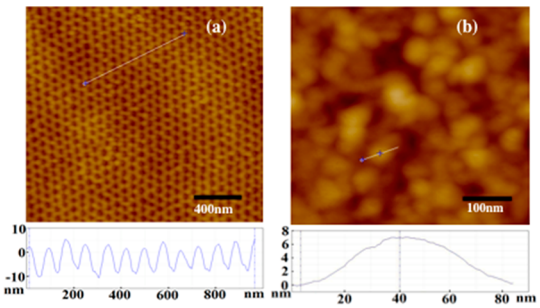

Figure 9. (a) AFM height image of the PS-*b*-P4VP nanoporous membrane; (b) after exposure to BHb solution at the physiological pH of 7.4.

carried negative surface charges, which caused the strong electrostatic attraction and adsorption on the charged membrane at low ionic strength. Because the electrostatic interactions between the proteins and charged membranes occurred across the entire thickness of the modified membrane, not only at its surface did it offer an efficient electrostatic interaction region for separation. Moreover, even when BSA and the nanopores had opposite charge, a distortion of the electric double layer around the charged protein caused by the charged pores could lead to a net repulsive interaction, which would also hinder the transport of BSA.

The modified charged membranes effectively enhanced the selectivity of the two similarly sized proteins and acted as molecular "on−off" gates, where the "on" position for high molecular transport occurred at the pI. By optimizing the membrane with quaternization, we successfully tailored it to exclude one protein completely while permitting the transport of the other.

It is possible that reversible adsorption of charged protein plays a role in protein transport. For instance, BHb is negatively charged at the physiological pH of 7.4 and will be adsorbed on the surface of the positively charged membrane. SEM images show a "clean" membrane before exposure to the protein solution (Figure 9a) and another membrane after the experiment at pH 7.4 (Figure 9b). The vertical distance measured with AFM was about 6.9 nm. This size closely matches the longest dimension of a single BHb molecule (6.4 nm × 5.5 nm × 5 nm) and indicates that there was a monolayer of the protein adsorbed on the surface. Such adsorption tends to reduce the effective pore size (Figure 10) during diffusion.

This reversible adsorption could be used for protein drug delivery since the nanoporous membrane contains innumerable cylinders that are like millions of micro affinity columns. After the diffusion experiments, the membranes were rinsed with ultrapure water and soaked

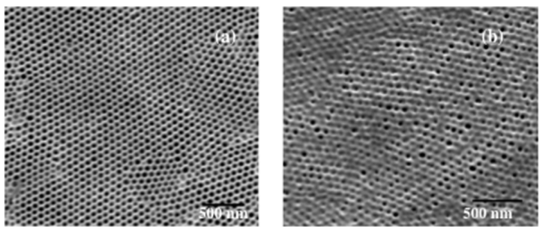

Figure 10. SEM images of (a) the quaternized PS-*b*-P4VP nanoporous membrane; (b) after exposure to protein solution.

in a buffer solution at pH 4.7, where BHb is positively charged. BHb was then released from the membrane. After the treatment, the pore radius of the membranes did not change as observed from water flow experiments, indicating that there was no irreversible protein adsorption inside the pores. If irreversible protein adsorption took place, the adsorbed protein would partially block the pore and cause a decrease in water flux.

CONCLUSIONS

This study represents the first use of a PS-*b*-P4VP membrane for selective separation of proteins. Our membrane is useful not only for size-based separations but also for separation of similarly sized molecules with different charge states.

First, the permeation ratio of BSA to IgG (over 87) suggests that our membrane can be used for membrane-based protein fractionation or chromatography, because it allows for recovery of both the retentate and the filtrate fractions. Second, the membrane can efficiently separate similarly sized proteins (BSA and BHb) at pH 4.7. Finally, by quaternization we can fashion a membrane that acts as a molecular "on−off" gate for similarly sized proteins, where the "on" position for protein transport occurs at the protein's pI. We successfully tailored this membrane for the total exclusion of one protein while allowing the transport of another. Our focus in this work was on diffusion to help us to understand the transport behaviors and separation mechanism of the biomolecules through the membrane. Although the diffusion rates were not very high when the ionic strength and pore sizes were reduced to enhance selectivity, substantial enhancement of the rate would be expected in a centrifuge or pressure-driven system since our membrane can withstand up to three bars of differential pressure. Such systems are able to achieve a desirable separation performance with both high selectivity and high rate. Our results demonstrate that asymmetric block copolymer membranes have unusual transport properties that can be optimized for efficient bioseparation applications.

EXPERIMENTAL SECTION

Membrane Preparation. Polystyrene-*b*-poly-4-vinylpyridine block copolymer (PS-*b*-P4VP, 175,000-*b*-65,000 g/mol) was obtained from Polymer Source, Inc. (Canada). *N*,*N*-Dimethyl formamide (DMF), tetrahydrofuran (THF), dioxane, and 2-chloroacetamide were purchased from Sigma Aldrich. Ultrapure Milli-Q water (18.2 MΩ) was used for preparation of all solutions and for rinsing. Membranes were cast from a polymer solution on glass plates, using casting blades with 200 μm gate height. The casting

solution contained 15 wt % copolymer, 28.3 wt % DMF, 28.3 wt % THF, and 28.3 wt % dioxane. The solvent was allowed to evaporate up to 10 s at room temperature, and the film was then immersed in a nonsolvent bath (water) at room temperature. The resulting films showed a nontransparent white color. Their morphology was examined by scanning electron microscopy (SEM) and atomic force microscopy (AFM).

Scanning Electron Microscopy. A small piece of wet membrane was dried under nitrogen gas and then placed on the specimen holder using carbon conductive tapes. To avoid charging problems, the samples were sputter coated with gold for 90 s at 5 mA current in an argon atmosphere. The samples were then transferred to an SEM stage and observed on FEI Quanta 600 and Helios 400S microscopes at 30 kV.

Atomic Force Microscopy. The AFM analysis was performed using an ICON Veeco microscope operating in the tapping mode under ambient conditions, using commercial silicon TM AFM tips (model MPP 12100). For observation of the nanoporous membrane surface morphology, a piece of wet membrane was dried under nitrogen gas and placed on a glass slide using carbon conductive tapes.

Water Flux and pH Response Characterization. The water flux was measured in a water permeation experiment under different pH values. The membranes (diameter 2.2 cm) were tested in an Amicon cell at a pressure of 1.38 bar. The same procedure was repeated, and the effective pore radius of this tunable membrane was estimated using Hagen−Poiseuille's law.

Quaternization of the PS-*b*-P4VP Membrane. In our quaternization procedure, wet membranes were immersed in aqueous solutions of 2-chloroacetamide at room temperature. Then the membranes were rinsed with MQ water to remove the remaining quaternization agent on the surface. In our protein separation experiment, the membranes were all immersed in excess aqueous solutions of 2-chloroacetamide for 3 days to make sure that the P4VP was fully quaternized. After quaternization the membranes were positively charged. It is worth noting that the surface morphology of the membrane did not change before and after quaternization.

Protein Transport and Separation. Globulin-γ (150 kDa), bovine serum albumin (66 kDa), and bovine hemoglobin (65 kDa) are from Sigma Co. They were used as received with no further purification. A commercial solution of PBS (at the physiological pH of 7.4) was used after dilution in water (10 times). We used a diffusion cell (PermGear, Inc.) with two compartments (left and right chambers). The free-standing membrane was placed between the two chambers. The ordered top layer of the membrane was placed toward the left side. The effective permeation area of the membrane was 1.77 cm^2, and the volumes of the left and right chambers were 7.0 mL each. The left chamber was filled with a buffer solution mixed with protein, and the right chamber contained a blank buffer solution initially without protein. Both chambers were stirred vigorously by using two magnetic stirrers and a stirring plate. The same stirring speed was maintained during all experiments. PBS solutions with different external pH and low ionic strength ($I = 0.01$ M) were used in the diffusion experiments. All the buffer solutions are adjusted to desired pH values by mixing different amounts of potassium dihydrogen phosphate (KH_2PO_4) and disodium hydrogen phosphate (Na_2HPO_4) (both from Fluka) in Milli-Q water and are used within three days of preparation. The pH values were confirmed with a pH meter. The initial concentration of protein in the left cell was 1.0 mg/mL. Every 30 min a measurement was taken. Samples of the permeate at different times were collected and stored at −20 °C until further analysis. In the single protein transport, the protein concentration in the right chamber was measured with an UV−visible spectrophotometer at 590 nm using a Bradford assay. In the mixed protein separation experiments, the initial concentrations of BHb and BSA in the left chamber were 1.0 mg/mL each. The protein concentration in the right chamber was determined by a NanoDrop 2000/2000c spectrophotometer (Thermo Fisher Scientific). It is well known that BHb in solution displays two absorbance maxima at two different wavelengths, around 280 and 405 nm, whereas the BSA in solution exhibits only one absorbance maximum, at 280 nm. Therefore, the BHb *versus* concentration in the protein mixture was obtained directly from the absorbance at 405 nm. The BSA concentration at 280 nm was calculated by subtracting the BHb contribution (evaluated from the BHb concentration) at this position from the total absorbance at 280 nm. The fluxes of the proteins across the membrane (F_{BSA} and F_{BHb}) were obtained from the slopes of the protein concentrations in the right chamber time.

Polyacrylamide Gel Electrophoresis (PAGE) Analysis and Gel Staining. Laemmli (SDS-PAGE) sample loading buffer, 10× Tris/glycine/SDS electrophoresis migration buffer, 4−20% Mini-PROTEAN TGX Precast Gel, Precision Plus Protein Unstained Standards (10−250 kD), and Bio-Safe colloidal Coomassie Brilliant Blue G-250 protein staining solution were purchased from Bio-Rad (USA). One part of the sample was diluted with one part of the Laemmli sample buffer. The sample solution was heated at 70 °C for 10 min before gel loading. The SDS-PAGE was then carried out on a 4−20% precast polyacrylamide gel in a Mini-PROTEAN Tetra Cell (Bio-Rad, USA). The migration of the proteins occurred at a constant voltage of 100 V with initial current of 20 mA/gel and at 1 W for about 1.5 h in migration buffer. After electrophoresis, the gel was stained with colloidal Coomassie Blue G250 for 2 h with gentle agitation and then washed in Milli-Q water until the background was clear.

Conflict of Interest: The authors declare no competing financial interest.

Acknowledgment. The work was supported by the KAUST Seed-Fund Project "Isoporous Membranes". We thank Lan Zhao from Advanced Nanofabrication, Imaging and Characterization Lab at KAUST for her help with the morphological characterization.

REFERENCES AND NOTES

1. Latulippe, D. R.; Ager, K.; Zydney, A. L. Flux Dependent Transmission of Supercoiled Plasmid DNA through Ultrafiltration Membranes. *J. Membr. Sci.* **2007**, *294*, 169–177.
2. Van Reis, R.; Zydney, A. Bioprocess Membrane Technology. *J. Membr. Sci.* **2007**, *297*, 16–50.
3. de Vos, R. M.; Verweij, H. High-Selectivity, High-Flux Silica Membranes for Gas Separation. *Science* **1998**, *279*, 1710–1711.
4. Li, K. *Ceramic Membranes for Separation and Reaction*; John Wiley & Sons, 2007; Chapter 1.
5. Striemer, C. C.; Gaborski, T. R.; McGrath, J. L.; Fauchet, P. M. Charge- and Size-Based Separation of Macromolecules Using Ultrathin Silicon Membranes. *Nature* **2007**, *445*, 749–753.
6. Tong, H. D.; Janson, H. V.; Gadgil, V. J.; Bostan, C. G.; Berenschot, E.; Elwenspoek, M. Silicon Nitride Nanosieve Membrane. *Nano Lett.* **2004**, *4*, 283–287.
7. Létant, S. E.; Van Buuren, T. W.; Terminello, L. J. Nanochannel Arrays on Silicon Platforms by Electrochemistry. *Nano Lett.* **2004**, *4*, 1705–1707.
8. Li, L.; Schulte, L.; Clausen, L. D.; Hansen, K. M.; Jonsson, G. E.; Ndoni, S. Gyroid Nanoporous Membranes with Tunable Permeability. *ACS Nano* **2011**, *5*, 7754–7766.
9. Furneaux, R. C.; Rigby, W. R.; Davidson, A. P. The Formation of Controlled-Porosity Membranes from Anodically Oxidized Aluminum. *Nature* **1989**, *337*, 147–149.
10. Vandezande, P.; Gevers, L. E. M.; Vankelecom, I. F. J. Solvent Resistant Nanofiltration: Separating on a Molecular Level. *Chem. Soc. Rev.* **2008**, *37*, 365–405.
11. Yamaguchi, A.; Uejo, F.; Yoda, T.; Tanamura, Y.; Yamashita, T.; Teramae, N. Self-Assembly of a Silica-Surfactant Nanocomposite in a Porous Alumina Membrane. *Nat. Mater.* **2004**, *3*, 337–341.
12. Lee, S. B.; Martin, C. R. Electromodulated Molecular Transport in Gold-Nanotube Membranes. *J. Am. Chem. Soc.* **2002**, *124*, 11850–11851.
13. Torres, M. R.; Ramos, A. J.; Soriano, E. Ultrafiltration of Blood Proteins by Experimental Polyamide Membranes. *Bioprocess Eng.* **1998**, *19*, 213–215.
14. Pujar, N. S.; Zydney, A. L. J. Electrostatic Effects on Protein Partitioning in Size Exclusion Chromatography and Membrane Ultrafiltration. *J. Chromatogr. A* **1998**, *796*, 229–238.

15. Koehler, J. A.; Ulbricht, M.; Belfort, G. Intermolecular Forces between Proteins and Polymer Films with Relevance to Filtration. *Langmuir* **1997**, *13*, 4162–4171.
16. Saksena, S.; Zydney, A. L. Influence of Protein-Protein Interactions on Bulk Mass Transport in Ultrafiltration. *J. Membr. Sci.* **1997**, *125*, 93–108.
17. Osmanbeyoglu, H. U.; Hur, T. B.; Kim, H. K. Thin Alumina Nanoporous Membranes for Similar Size Biomolecule Separation. *J. Membr. Sci.* **2009**, *343*, 1–6.
18. Chun, K. Y.; Stroeve, P. Protein Transport in Nanoporous Membranes Modified with Self-Assembled Monolayers of Functionalized Thiols. *Langmuir* **2002**, *18*, 4653–4658.
19. Ku, J.; Stroeve, P. Protein Diffusion in Charged Nanotubes: "On-Off: Behavior of Molecular Transport. *Langmuir* **2004**, *20*, 2030–2032.
20. Peinemann, K.-V.; Abetz, V.; Simon, P. F. W. Asymmetric Superstructure Formed in a Block Copolymer *via* Phase Separation. *Nat. Mater.* **2007**, *6*, 992–996.
21. Nunes, S. P.; Karunakaran, M.; Pradeep, N.; Behzad, A. R.; Hooghan, B.; Sougrat, R.; He, H.; Peinemann, K.-V. From Micelle Supramolecular Assemblies in Selective Solvents to Isoporous Membranes. *Langmuir* **2011**, *27*, 10184–10190.
22. Nunes, S. P.; Sougrat, R.; Hooghan, B.; Anjum, D. H.; Behzad, A. R.; Zhao, L.; Pradeep, N.; Pinnau, I.; Vainio, U.; Peinemann, K.-V. Ultraporous Films with Uniform Nanochannels by Block Copolymer Micelles Assembly. *Macromolecules* **2010**, *43*, 8079–8085.
23. Nunes, S. P.; Behzad, A. R.; Hooghan, B.; Sougrat, R.; Karunakaran, M.; Pradeep, N.; Vainio, U.; Peinemann, K.-V. Switchable pH-Responsive Polymeric Membranes Prepared *via* Block Copolymer Micelle Assembly. *ACS Nano* **2011**, *5*, 3516–3522.
24. Li, Q. Y.; Cui, Z. F.; Pepper, D. S. Fractionation of HSA and IgG by Gas Sparged Ultrafiltration. *J. Membr. Sci.* **1997**, *136*, 181–190.
25. Ghosh, R.; Cui, Z. F. Fractionation of BSA and Lysozyme Using Ultrafiltration: Effect of pH and Membrane Pretreatment. *J. Membr. Sci.* **1998**, *139*, 17–28.
26. van Eijndhoven, H. C. M.; Saksena, S.; Zydney, A. L. Protein Fractionation Using Membrane Filtration: Role of Electrostatic Interactions. *Biotechnol. Bioeng.* **1995**, *48*, 406–414.
27. Squires, T. M.; Quake, S. R. Microfluidics: Fluid Physics at the Nanoliter Scale. *Rev. Mod. Phys.* **2005**, *77*, 977–1026.
28. Bicak, N.; Gazi, M. Quantitative Quaternization of Poly-(4-Vinyl Pyridine). *J. MacromoL. Sci. A* **2003**, *40*, 585–591.
29. Cirello-Egamino, J.; Brindle, I. D. Determination of Chloride Ions by Reaction with Mercury Thiocyanate in the Absence of Iron(III) Using a UV-photometric, Flow Injection Method. *Analyst* **1995**, *120*, 183–186.
30. Bicak, N.; Sonmez, H. B. Quaternization of Poly(4-Vinyl Pyridine) Beads with 2-Chloroacetamide for Selective Mercury Extraction. *React. Funct. Polym.* **2002**, *51*, 55–60.